Antioxidant Poly(lactic-*co*-glycolic) Acid Nanoparticles Made with α-Tocopherol–Ascorbic Acid Surfactant

Carlos E. Astete,[†] Debra Dolliver,[‡] Meocha Whaley,[†] Lavrent Khachatryan,[§] and Cristina M. Sabliov[†,*]

[†]Biological and Agricultural Engineering Department, Louisiana State University Agricultural Center, United States, [‡]Chemistry-Physics Department, Southeastern Louisiana University, United States, and [§]Chemistry Department, Louisiana State University, United States

ABSTRACT The goal of the study was to synthesize a surfactant made of α-tocopherol (vitamin E) and ascorbic acid (vitamin C) of antioxidant properties dubbed as EC, and to use this surfactant to make poly(lactic-*co*-glycolic) acid (PLGA) nanoparticles. Self-assembled EC nanostructures and PLGA–EC nanoparticles were made by nanoprecipitation, and their physical properties (size, size distribution, morphology) were studied at different salt concentrations, surfactant concentrations, and polymer/surfactant ratios. EC surfactant was shown to form self-assembled nanostructures in water with a size of 22 to 138 nm in the presence of sodium chloride, or 12 to 31 nm when synthesis was carried out in sodium bicarbonate. Polymeric PLGA–EC nanoparticles presented a size of 90 to 126 nm for 40% to 120% mass ratio PLGA to surfactant. For the same mass ratios, the PLGA–Span80 formed particles measured 155 to 216 nm. Span80 formed bilayers, whereas EC formed monolayers at the interfaces. PLGA–EC nanoparticles and EC showed antioxidant activity based on 2,2-diphenyl-1-picrylhydrazyl (DPPH) radical scavenging assay measurements using UV and EPR techniques, antioxidant activity which is not characteristic to commercially available Span80. The thiobarbituric acid reactive substances (TBARS) assay for lipid peroxidation showed that PLGA nanoparticles with EC performed better as antioxidants than the EC nanoassembly or the free vitamin C. Nanoparticles were readily internalized by HepG2 cells and were localized in the cytoplasm. The newly synthesized EC surfactant was therefore found successful in forming uniform, small size polymeric nanoparticles of intrinsic antioxidant properties.

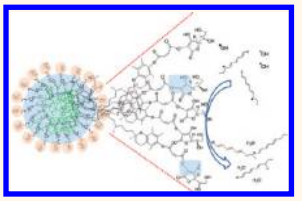

KEYWORDS: PLGA nanoparticles · nanoprecipitation · surfactant · antioxidant · vitamin E · vitamin C

Polymeric nanoparticles have been extensively researched as delivery systems of different active components such as anticancer drugs, vitamins, proteins, peptides, and others.[1–6] The advantages are numerous. Polymeric nanoparticles protect the drug against degradation while releasing it in a controlled manner which translates into lower toxicity and less side effects. Also, drug targeting can be achieved by surface attachment of moieties of specific interaction with the target (*i.e.*, proteins, peptides, folic acid, and lectins).[7–11] Despite these advantages, polymeric nanoparticles, in and of themselves, do not provide any benefit in the treatment of disease, but rather, they act as carriers for the drug. Nanoparticles with inherent properties, such as antioxidant activity, could be useful in treating oxidative-stress related diseases such as atherosclerosis and cancer, in addition to playing their obvious role as vehicles for drug transport and delivery.

Antioxidant nanoparticles with promising characteristics for the treatment of diseases related with oxidative damage have been built already. The current approach is mainly based on the entrapment of an antioxidant agent into the polymeric matrix to be protected and transported by the bloodstream. The antioxidant action is due to the release of the antioxidant agent entrapped in the polymeric matrix. In general, better antioxidant action is seen when the antioxidant is entrapped in a polymeric matrix relative to other modes of delivery. For example, SOD entrapped in PLGA nanoparticles were able to provide better protection to human neurons (100% cell survival for 6 h) compared to SOD in solution (25% cell survival) and pegylated SOD (PEG-SOD) (40% cell survival) at a SOD dose of 100 U or higher.[12] Another study showed that entrapped melatonin in poly(methacrylic acid-*co*-methyl methacrylate) nanoparticles had better antioxidant protection compared with melatonin in solution at doses of 1 mg/kg and 10 mg/kg.[13] The entrapment of catalase (an enzyme that dissociates hydrogen peroxide into water and oxygen) into poly(ethylene glycol (PEG) nanocarriers (spheres and filaments) by

* Address correspondence to csabliov@lsu.edu.

Received for review October 21, 2010 and accepted October 21, 2011.

Published online October 21, 2011
10.1021/nn102845t

© 2011 American Chemical Society

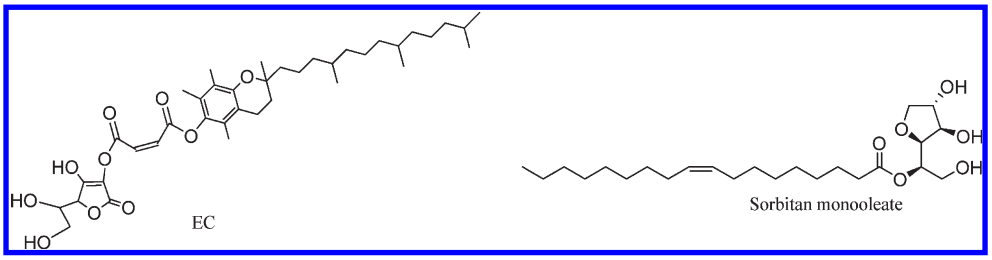

Figure 1. Chemical structure of EC (α-tocopherol−ascorbic acid) and Sorbitan monooleate (Span80).

double emulsion was performed by Simone *et al*. with the purpose of promoting its resistance to proteases attack for an enhanced catalase activity. The catalase entrapped in nanoparticles was more resistant to proteases attack.[14]

Besides entrapping an antioxidant in polymeric nanoparticles, nanoparticle systems of intrinsic antioxidant properties could be built by virtue of covalently linking an antioxidant to the nanoparticle or by attaching an antioxidant agent to inorganic nanoparticles. Williams *et al*. conjugated PEG with gluthatione (scavenger of hydroxyl radicals, superoxide radicals, singlet oxygen) to form self-assembled nanoparticles and showed that the glutathione−PEG nanoparticle protected the human brain neuroblastoma cells against oxidative damage at comparable levels with free glutathione.[15] Another approach used by Nie *et al*. was to synthesize surface-functionalized gold nanoparticles with synthetic antioxidant Trolox (water-soluble vitamin E analogue). The data collected suggested that gold−Trolox nanoparticles with a mean size of 4.5 ± 0.7 nm were better antioxidants than Trolox in solution.[16] In a different attempt to create nanoparticles of inherent antioxidant properties, the antioxidant α-lipoic acid was covalently conjugated to obtain multiple molecules of different hydrophilicities which assembled into 200−600 nm nanoparticles (as a function of hydrophobicity) synthesized by nanoprecipitation. Again, nanoparticles showed an increased antioxidant activity as compared with α-lipoic acid in solution.[17]

In this study, natural antioxidant molecules, α-tocopherol (vitamin E) and ascorbic acid (vitamin C) were used to create a new surfactant (EC) of antioxidant properties to be used in polymeric nanoparticle synthesis. Vitamin E is hydrophobic and vitamin C is hydrophilic, thus when the two are linked, an amphiphilic EC surfactant results. The selection of the two components was based on compelling information that vitamins E and C are some of the most potent natural antioxidants. Vitamin E is a main chain breaking agent of radical reactions (*i.e.*, lipid peroxidation) protecting hydrophobic molecules against reactive oxygen radicals (ROS);[18−21] α-tocopherol acts mainly against peroxyl radicals and perhydroxyl radicals with a rate constant of 2×10^5 M^{-1} s^{-1}.[22] On the other hand, at physiological pH, vitamin C interacts with α-tocopheroxyl radical to regenerate α-tocopherol suggesting a synergetic effect between the two molecules (rate constant of 1.5×10^6 M^{-1} s^{-1}).[22,23] Vitamin C reacts with perhydroxyl radicals at a rate constant of 1.6×10^4 M^{-1} s^{-1};[22,23] it prevents damage by peroxynitrate and acts as a scavenger of hydroxyl radical, hypochlorous acid, thiyl, sulphenyl radicals, and others.[24]

Vitamin C and vitamin E derivatives have been synthesized in the past as new synthetic antioxidants in an attempt to improve the antioxidant properties of the starting vitamin, or to form new surfactants.[25−35] It was our goal not only to synthesize a novel surfactant of antioxidant properties from vitamin E and vitamin C, but to also form self-assembled nanostructures as well as polymeric nanoparticles in the presence of the newly synthesized EC surfactant. The nanostructures were characterized in terms of size, polydispersity, morphology, stability, and antioxidant activity and were compared with nanostructures formed under similar conditions in the presence of Span80 as a surfactant.

RESULTS AND DISCUSSION

EC exhibited poor water solubility, but it was soluble in polar solvents such as acetone. Upon the addition of the organic phase with dissolved EC or Span80 to water and subsequent diffusion and evaporation of acetone, water dispersions of self-assembled EC and Span80 formed. In the presence of PLGA, polymeric nanoparticles stabilized by the surfactant (EC or Span80, Figure 1) were formed by a modified version of nanoprecipitation.[36] The effect of salts and surfactant concentration on the size of nanostructures formed from pure EC and Span80 surfactants was studied. Next, polymeric particles with PLGA and each surfactant were made, and the effect of surfactant/PLGA ratio on nanoparticle size and polydispersity was assessed. Finally, a mixture of EC and Span 80 was used to analyze the effect of EC/Span80 ratio on PLGA particle size and polydispersity.

Nanostructures Formed by Self-Assembly of EC and Span80—Effect of Type and Salt Concentration. The effect of the type and concentration of salts present in the aqueous phase on the size and polydispersity of the nanostructures formed by EC and Span80 surfactants was studied (Figure 2). The EC nanostructures formed in an aqueous solution of sodium bicarbonate showed a

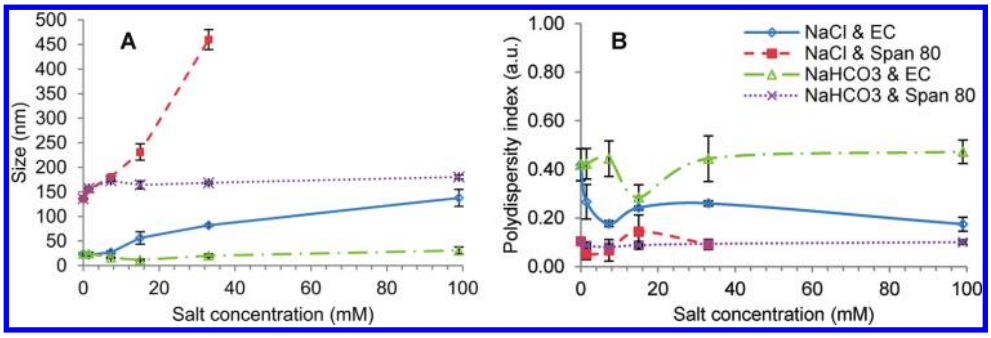

Figure 2. Effect of salt concentration on the size and polydispersity of Span80 and EC nanostructures: (a) nanostructure diameter and (b) polydispersity index for Span80 and EC self-assembled nanostructures in sodium bicarbonate and sodium chloride aqueous solutions.

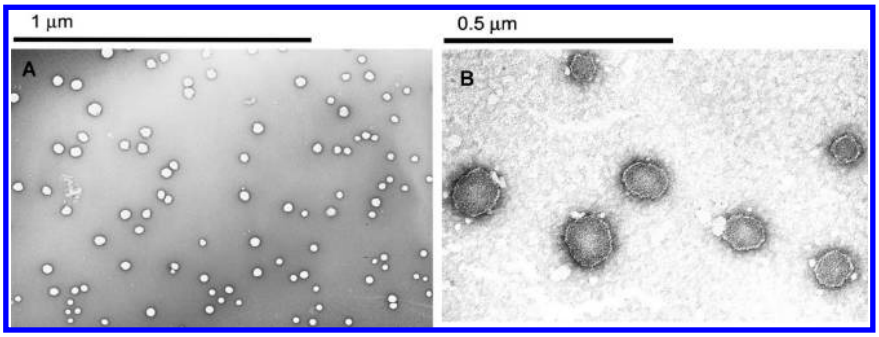

Figure 3. (A) TEM picture of EC surfactant in sodium chloride solution at 66×. The sample was prepared with 2% uracyl acatate. (B) TEM picture of Span80 self-assembled nanostructure in sodium bicarbonate solution. Note: Contrast was enhanced by adding gold nanoparticles (4 nm Sigma Aldrich, 50 μL) to the organic phase in a concentration of 0.1 mg/mL prior to the TEM analysis as described in the methodology section.

smaller particle size (Figure 2A) as compared to the size of the nanostructures formed in the presence of sodium chloride. The EC nanoparticles ranged between 17 and 31 nm for the salt concentrations studied (0−100 mM). In contrast, the polydispersity index (>0.5) was higher for these particles as compared to that of particles made in the presence of NaCl (Figure 2B).

The EC nanostructures synthesized in the presence of sodium chloride showed a mean size of 22−138 nm in diameter with a polydispersity index that ranged from 0.18 to 0.27. The tendency was for the size to increase as the salt concentration increased from 0 to 100 mM. The size growth was expected because the aggregation number increases and critical micelle concentration (cmc) decreases as a function of salt added, which results in an increased size.[37,38] The samples synthesized with sodium bicarbonate presented the smaller nanostructure size, from 17 ± 2 to 31 ± 7 nm, with a minimum nanostructure size at 15 mM sodium bicarbonate. The difference in nanostructure size between nanoparticles synthesized in the presence of sodium chloride and sodium bicarbonate is attributed to the lack of water available to the surfactant in the presence of chloride ions. Chloride ions, when added to the solution, hydrate and under these conditions, ionic surfactants such as EC undergo morphology changes, largely dependent on the number of water molecules surrounding the headgroups.[39] Sodium bicarbonate was therefore found more suitable for formation of smaller nanostructures. The highest polydispersity index values for all nanostructures occurred at the lowest salt concentration tested (1.5 mM).

The nonionic Span80 self-assembled into bigger nanostructures as compared to EC. When synthesized in an aqueous solution of sodium bicarbonate, the mean Span80 particle size ranged from 157 to 182 nm (Figure 2). The polydispersity index obtained varied between 0.05 and 0.14. At the lower salt concentration monodisperse Span80 nanostructures, represented by a polydispersity index value lower than 0.1, were formed. The Span80 samples synthesized in the presence of sodium chloride showed an increase in the particle size as a function of salt concentration. Moreover, the nanostructures synthesized with 99 mM sodium chloride in the aqueous phase presented phase separation following the evaporation of acetone. The presence of chloride and sodium ions at high concentrations promoted less hydrogen-bond interactions with the OH groups of Span80, and the salting out process was responsible for the observed precipitation.

The TEM pictures revealed that spherical-shaped EC nanostructures were formed when sodium chloride was used in the aqueous phase (Figure 3). The size observed by TEM was in agreement with the DLS data and suggested a reduced aggregation and more

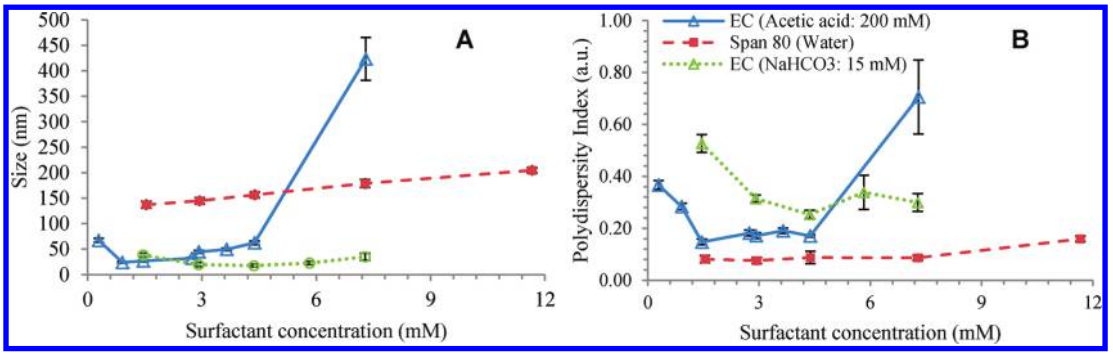

Figure 4. (A) Size and (B) polydispersity index of nanostructures synthesized at different EC and Span80 surfactant concentrations.

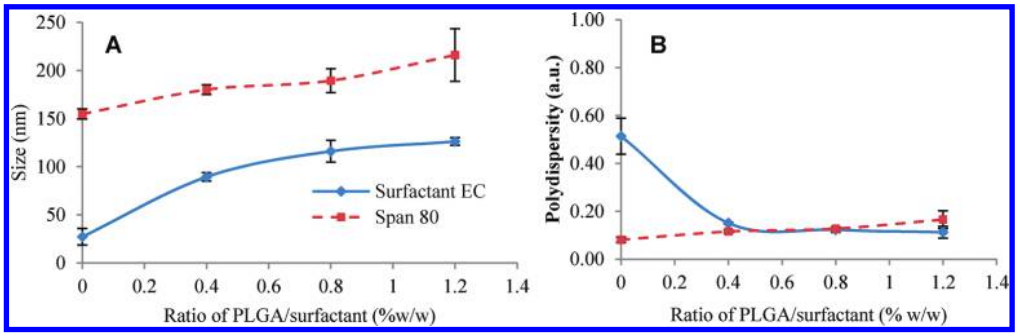

Figure 5. Size (A) and polydispersity (B) of polymeric PLGA nanoparticles synthesized with surfactant EC and Span80.

uniform particle size. Contrary to EC (Figure 3A), hydrophobic Span80 had a tendency to form bilayers similar to those formed by phospholipids, a tendency which reflected in the bigger size of the Span80 nanostructures and their smaller polydispersity index (Figure 3B).

Nanostructures Formed by Self-Assembly of EC and Span80-Effect of Surfactant Concentration. The particle size increased with an increase in the concentration of the surfactant for both EC and Span80. The polydispersity of self-assembled EC and Span80 (nonionic surfactant) increased as well, as the concentration of the components increased (Figure 4). The EC nanostructures showed a particle size that did not change at low surfactant concentrations (1−5 mM), but at concentrations exceeding 5 mM the size of the EC nanostructures increased sharply in acetic acid due to protonation of the −OH group of the EC at acidic pH values and decrease in the hydrophilicity of the surfactant (Figure 4A). The increase in the amount of EC promoted aggregation, which reflected in the high values of the polydispersity index (Figure 4B) for the sample with acetic acid (0.749 for 7.3 mM of EC). At lower EC concentrations of 1.5−4.4 mM the polydispersity values were 0.15−0.17, which indicated formation of monodisperse suspensions. The samples with sodium bicarbonate were more stable, but the particle size increase was observed still at a 7.3 mM EC. The particles synthesized in sodium bicarbonate presented a higher polydispersity value (0.51−0.24) in the 1.5−4.4 mM EC concentration range. At an EC concentration of 7.3 mM, the polydispersity was smaller (0.28) as compared to that of the sample formed in acetic acid (0.75). The particles synthesized with Span80 without salt in the aqueous phase showed bigger particle size than the EC particles, with a stable particle size increase as the surfactant concentration was increased between 141 and 265 nm for 1.5 to 23.3 mM of Span80. The polydispersity showed a stable increment from 0.07 to 0.34. Higher concentrations presented phase separation in which Span80 was no longer able to form nanostructures.

PLGA Nanoparticles synthesized with EC and Span80 Surfactants—Effect of PLGA/Surfactant Ratio. The PLGA−EC nanoparticles presented a mean size ranging from 54 to 130 nm (Figure 5) as a function of the amount of PLGA entrapped in the core; the tendency was for the nanoparticle size to increase as the amount of PLGA increased. The size was relatively uniform over the different PLGA concentrations used. The addition of PLGA to the EC nanostructures did not increase aggregation, and the structures were more uniform compared with those formed by EC alone. The polydispersity index varied from 0.11 to 0.15. PLGA promoted a more stable EC particle by adding a hydrophobic core which interacted with the hydrophobic tail of vitamin E present in the EC surfactant. The PLGA nanoparticles synthesized with Span80 presented a bigger size in comparison with the PLGA−EC nanoparticles, and ranged from 155 to 216 nm. The polydispersity index was similar to that of the PLGA−EC nanoparticles (0.12−0.17). The

zeta potential of EC–PLGA nanoparticles significantly decreased ($p < 0.05$) with the addition of PLGA from -43.5 ± 9.4 to -71.9 ± 3.5 mV for 0 to 1.2 PLGA/surfactant w/w ratios. When PLGA nanoparticles were formed with Span80, the zeta potential did not significantly change from -61.2 ± 5.0 to -63.8 ± 12.0 mV for 0 to 1.2 PLGA/surfactant w/w ratios (Figure 6). Both systems presented negative zeta potential values at the tested pH of 8.4. The decrease of zeta potential for EC–PLGA nanoparticles with the addition of PLGA suggested that PLGA carboxylic end groups (COO^- at pH 8.4) promoted a drop in zeta potential. For Span80–PLGA nanoparticles, the addition of PLGA did not change the zeta potential and two different systems (Span80 vesicles, and PLGA–Span80) were formed, as observed in the TEM pictures (Figure 7).

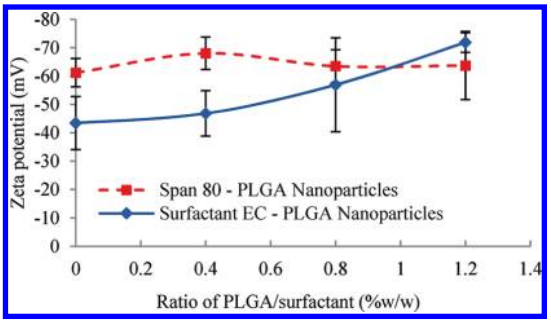

Figure 6. Change of zeta potential of EC–PLGA and Span80–PLGA nanoparticles with the addition of PLGA at pH 8.4 ($n = 3$).

TEM pictures (Figures 7) of polymeric PLGA nanoparticles synthesized with EC and span 80 showed that the EC–PLGA nanoparticles presented a uniform size distribution with limited aggregation (Figure 7A). The PLGA core promoted a uniform anchor to the hydrophobic vitamin E moiety of EC surfactant. The vitamin C moiety most likely placed itself at the interphase, facing the aqueous environment, and allowing particle suspension in water. The PLGA–Span80 nanostructures were less uniform in size as exhibited by the TEM pictures (Figure 7B). The sample showed a mixture of two different structures, one formed of Span80 alone, gray in appearance, in the form of vesicles (similar to those presented in Figure 3B), and nanoparticles with PLGA and Span80, depicted by the white circles.

Synthesis of PLGA Nanoparticles with a Mixture of EC and Span80. The effect of using a mixture of different Span80 to EC ratios on the PLGA particle size and polydispersity was evaluated (Figure 8). The tendency was for the particle size to increase when more Span80 was added to the mixture. Conversely, the polydispersity tended to decrease to values specific to monodisperse suspensions (polydispersity < 0.1) with the

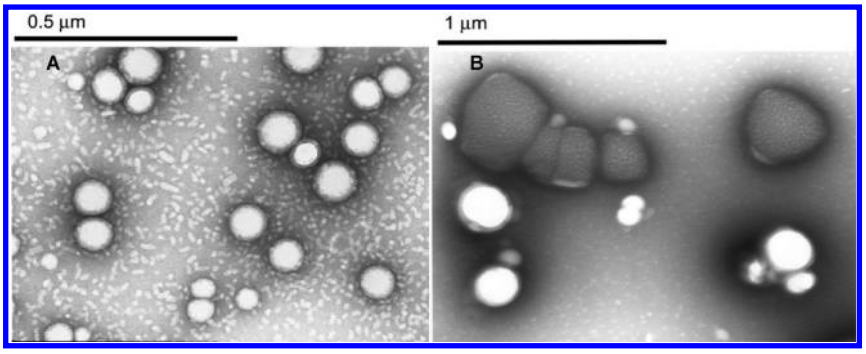

Figure 7. (A) PLGA–EC nanoparticles (ratio PLGA to EC was 0.8 to 1) in sodium bicarbonate (15 mM) with a magnification 100×. The EC concentration used was 1 mg/mL. (B) PLGA-Span80 nanoparticles (ratio PLGA to EC was 0.8 to 1) in $NaHCO_3$ (15 mM); two types of nanostructures are present, PLGA-Span80 (white structures) and Span80 vesicles (gray structures), magnification, 50×.

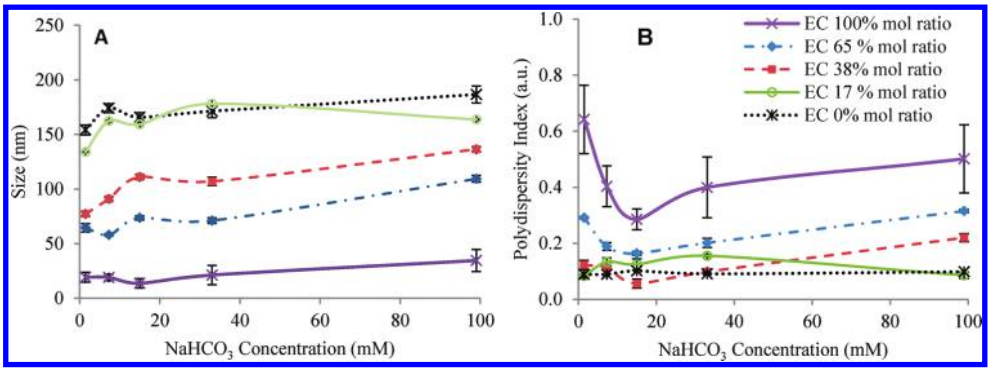

Figure 8. (A) Size and (B) polydispersity index values for PLGA polymeric nanoparticles synthesized with a mixture of EC and Span80 surfactants.

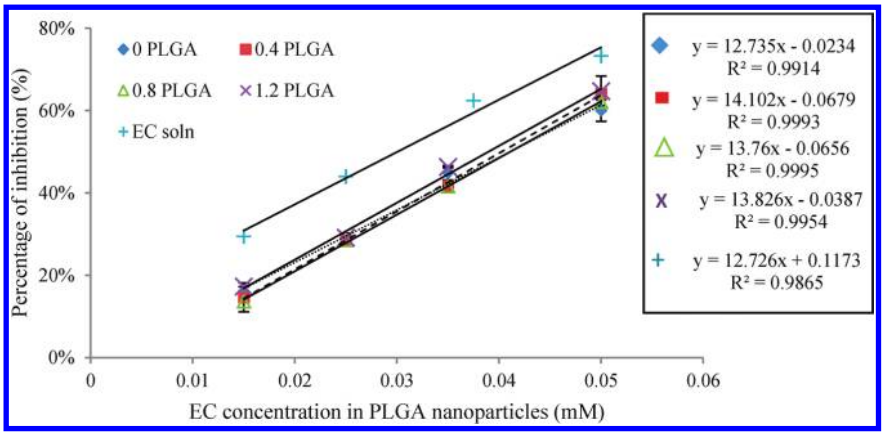

Figure 9. Rate of radical inhibition of PLGA–EC nanoparticles as a function of PLGA concentration as measured by the DPPH method.

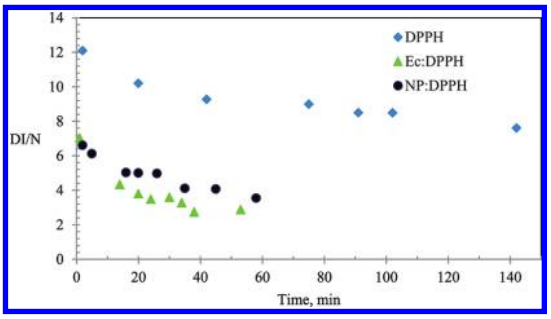

Figure 10. Scavenging of DPPH radicals by EC (triangles) and NP (black circles). Blue quadrates represent self-degradation of DPPH radicals as a reference. (DI/N value is the double integrated (DI) intensity of the EPR spectrum that has been normalized (N) to account for the conversion time, receiver gain, number of data points and sweep width [http://www.bruker-biospin.com/winepr.html?&L = 0]).

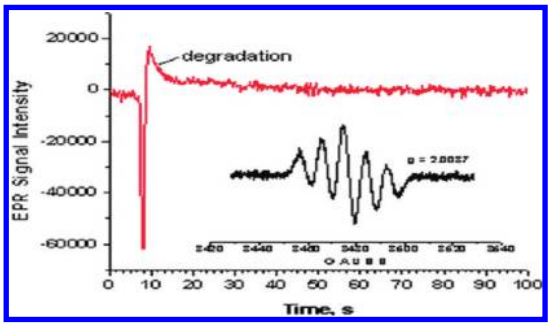

Figure 11. Time dependence of DPPH radical degradation (red line) in solution of NP (0.1 mM)/DPPH (0.1 mM) = 1:1 in EPR tube (diffusion regime). The inset shows the EPR spectrum of DPPH radicals with *g* value = 2.0037.

addition of more Span80. The data suggested that a reduction in the aggregation process promoted by the nonionic surfactant Span80 was achieved with the addition of the anionic EC surfactant, which promoted ionic repulsion and favored particle stabilization.

Antioxidant Properties of PLGA Nanoparticles Assessed by DPPH Assay. The DPPH radical scavenging assay was used to evaluate the antioxidant activity of PLGA–EC nanoparticles (PLGA–Span80 particles had no antioxidant activity). Linear regression was used to calculate the 50% inhibition of DPPH (Figure 9). The IC_{50} ranged from 30.6 to 37.4 μM for various PLGA concentrations, values which were not significantly different. The data suggested that the PLGA, size, and PI did not affect the antioxidant properties of the PLGA–EC nanoparticles with IC_{50} measuring 37.4 μM, 30.6 μM, 31.6 μM, and 33.4 μM for PLGA–EC particles made with polymer concentrations of 0 to 120% PLGA, respectively. The vitamin C moiety of the EC surfactant molecule contributed to the antioxidant activity of the polymeric antioxidant nanoparticle. The EC surfactant prepared with methanol–water (1:1 volume ratio) showed similar IC_{50} to the nanoparticles synthesized with EC (30.1 μM). The pure vitamin C and E showed IC_{50} values of 21.7 and 17.5 μM, respectively. The differences in IC_{50} between pure vitamin E and C with EC in solution and in nanoparticles were explained by the loss of an active OH group from ascorbic acid (vitamin C) and one OH group from α-tocopherol (vitamin E) during EC synthesis.

Electron Paramagnetic Resonance Measurements. The scavenging of the DPPH radical by EC or EC–NPs (an EPR spectrum of free DPPH radical is depicted in Figure 11) was followed by measuring the decrease in the EPR signal intensity, DI/N, Figure 10 (triangles for NP and circles for EC). The free DPPH radicals degraded at a noticeable rate during first 30–40 min, stabilizing at a value of DI/N = ~8, and then degraded at a slower rate while the degradation of DPPH after 30 min is minimum (Figure 10). The degradation of DPPH radicals was remarkable in the presence of free EC or EC–NPs which was reflected in the strong decay in the first 1 to 2 min. The initial concentration of DPPH radicals dropped from DI/N = 12 units to ~7 units by scavenging either by free EC or EC-NPs. The DPPH radicals still interacted effectively with EC and EC-NPs after the initial 2 min of reaction time; degradation slowed down over time and ended in 50–60 min.

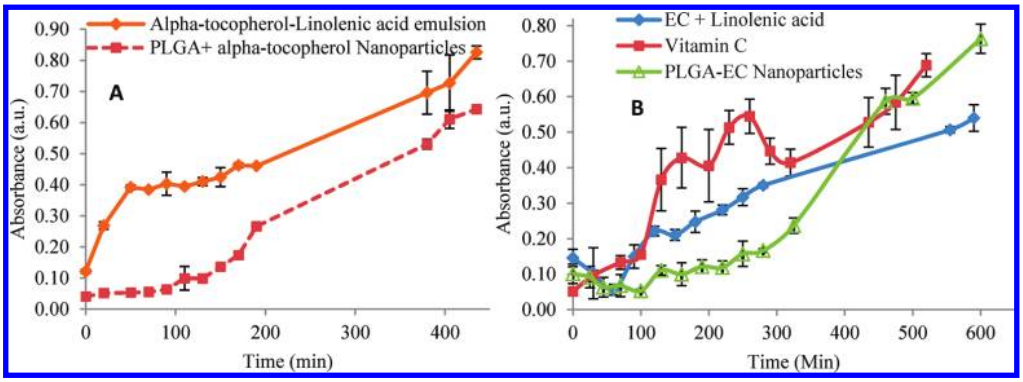

Figure 12. (A) α-Tocopherol (50 μM) was added in the organic phase, so it is mixed with linolenic acid, and PLGA-α-tocopherol nanoparticles were stabilized with polyvinyl alcohol (PVA). (B) EC mixed with linolenic acid (emulsion), PLGA−EC nanoparticles, and vitamin C added to linolenic acid emulsion (Tween 20) was studied at a concentration of 150 μM by TBARS assay.

A remarkable degradation of DPPH radicals occurred not over a 2 min span, but in fact during the first 5−6 s of mixing of EC or NP with DPPH. For instance, a rapid injection of DPPH solution into an EPR tube containing EC−NPs (or EC) solution showed a typical fast degradation curve, Figure 11 (top line), with ~40% of initial DPPH degraded during the first 5−6 s in the diffusion regime. For the comparison of antioxidant activity of organics in this region, where the reaction time is measured in seconds, a fast mixing technique must be applied.[16] Another alternative is to compare the scavenging activity of EC and EC−NPs over the time period, when the degradation rates of DPPH radicals are not fast and might be detected easily, for instance, between 2 and 10 min after mixing of the components (Figure 10). Using this approach, it was found that the antioxidant (scavenging) activity of EC was twice higher than that of EC−NPs (at the same EC concentration) when the maximum slopes were compared; for EC in relative units of intensity the slope was 0.21 units per minute *versus* 0.1 units per minute for EC−NPs. Therefore, the EPR measurements additionally supported that EC and EC−NPs exhibited antioxidant activity.

Three regions of interaction of DPPH with EC or EC−NPs were identified and used to account for different mechanisms of interaction between the antioxidant and DPPH over time. Within seconds, the antioxidant activity of free EC or EC−NPs was similar. Next, in the intermediate region between 2 and 10 min incubation, the activity of EC was almost twice higher in comparison with that of EC−NPs. During the slow region, at times longer than 10 min incubation, the activity of EC was comparable, but still superior to that of EC−NPs.

Antioxidant Properties of PLGA−EC, PLGA-α-tocopherol, and EC Nanoparticles Assessed by TBARS Assay. The TBARS assay was used to study the effect of EC nanoparticles and PLGA−EC nanoparticles in preventing lipid peroxidation. The model used was an emulsion made of linolenic acid with Tween 20, which was oxidized in the presence of a hydrophilic initiator 2,2′-azobis-2-methyl-propanimidamide dihydrochloride (AAPH). Three systems were studied. The first system was formed by adding EC directly in the organic phase, so the final nanostructure was formed by linolenic acid stabilized with EC antioxidant surfactant (both antioxidant and substrate physically colocalized). The second system consisted of polymeric nanoparticles synthesized with PLGA and EC added to the aqueous phase, so EC antioxidant surfactant was not in contact with the linolenic acid. The third system tested included vitamin C added to the aqueous phase (the antioxidant was not mixed in this case with linolenic acid). The control selected was α-tocopherol, a good hydrophobic natural antioxidant, in two forms: free (αα-tocopherol was mixed with linolenic acid), and α-tocopherol entrapped into the PLGA nanoparticles (α-tocopherol not mixed with linolenic acid). The PLGA nanoparticles with entrapped α-tocopherol were added in the aqueous phase for TBARS experiments. PLGA-Span80 particles did not show antioxidant activity, so were not tested in this experiment.

The inhibition of oxidative processes promoted by AAPH (hydrophilic initiator) was evaluated by comparing the lag phase in the different systems studied; the longer lag phase indicated a higher inhibition in formation of the thiobarbituric acid reactive species, or a higher antioxidant activity of the system studied.[40] PLGA nanoparticles with entrapped α-tocopherol performed better in protecting linolenic acid against oxidation as compared to the system with α-tocopherol mixed with linolenic acid (Figure 12A). The lag phase (time by which no oxidation byproduct were detected) was 100 min for the PLGA entrapped α-tocopherol nanoparticle system. In contrast, the system with α-tocopherol mixed with linolenic acid in an emulsion form showed an immediate increase in absorbance upon the addition of the initiator at the same concentration analyzed (50 μM). After the lag phase, both systems showed similar slopes in formation of the oxidation byproduct promoted by oxidation reactions

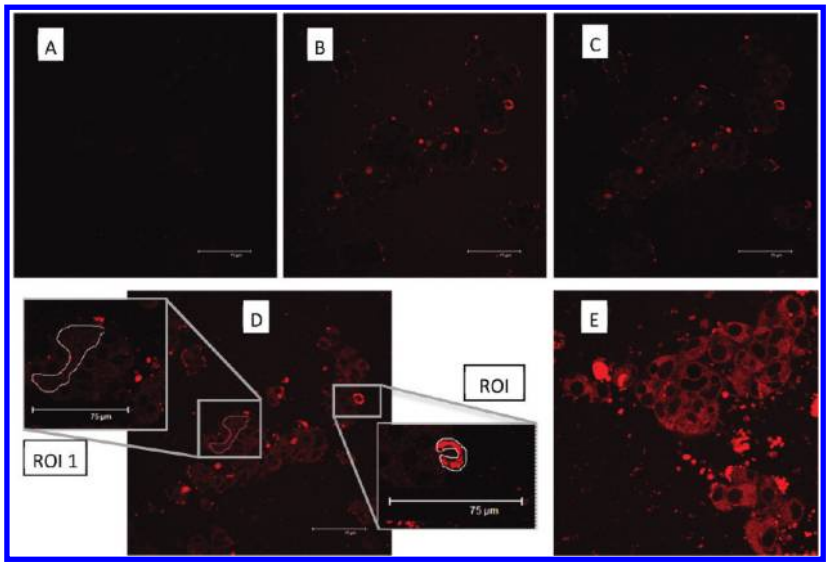

Figure 13. Fluorescent nanoparticles uptake by HepG2 cells: (A) preinoculation, (B) 0 min, (C) 5 min, (D) 60 min, and (E) 150 min. The excitation/emission used was 545/570 nm. ROI 1 shows the cell cluster selected for fluorescent measurements. ROI 2 shows an individual cell. Bars are 75 μm, picture E is 2×.

(lipid oxidation and final malondialdehyde formation) due to the consumption of antioxidant in the lag phase. The same trend was observed for the EC systems (Figure 12B). The PLGA–EC nanoparticles samples showed a lag phase of 240 min (minimum oxidation byproducts), compared with a constant increase of oxidation byproducts for the sample in the sample with vitamin C (where no lag phase was observed at the concentration tested, 150 μM). The samples with EC mixed with linolenic acid showed a lag phase of 70 min with a further constant slope increase. The TBARS assays data clearly suggested that the antioxidant action of EC and α-tocopherol against lipid peroxidation can be improved when the antioxidants were associated with PLGA polymeric nanoparticles.

The improved performance of the antioxidants (E and EC) in protecting lipids against oxidation when entrapped in polymeric PLGA nanoparticles could be explained by the pro-oxidant effect of the antioxidants which has been widely studied over the past decades.[41,42] Linolenic acid was shielded from the pro-oxidative effect of tocopheryl and ascorbyl radical byproduct formed as results of oxidative reactions from E and EC when these components were physically entrapped into polymeric nanoparticles. The pro-oxidant rate constant for α-tocopherol against limolenic acid in micelles had been estimated to 3.6×10^{-1} M^{-1} S^{-1}.[43] The vitamin C pro-oxidant effect had been related to the presence of metals such us copper and iron. The absence of tocopheryl or ascorbyl radical into the linolenic acid lipid phase minimized the generation of oxidative products which was reflected in longer lag phases for the PLGA nanoparticles with entrapped antioxidants as compared to that for the samples with mixed linolenic acid and antioxidants.

A second explanation of the improved antioxidant activity observed for both E and EC when entrapped in PLGA nanoparticles is related to the nanoparticle increased surface area and arrangement of the antioxidant molecules in these particles. Owing to close proximity of the hydrophilic groups (*i.e.*, hydroxyl groups) of the antioxidants, E or EC when in nanoparticle form may induce a lower pK_a of the phenols. The hydrogen bond donor conditions are improved in polar solvents under these conditions, promoting formation of ionic phenols which react faster with radicals by a process called sequential proton loss transfer as described by Nie *et al*. 2007, which worked with gold nanoparticle functionalized with Trolox moieties.[16] Hence, the PLGA–antioxidant system promoted faster reactions with AAPH radicals increasing the lag phase up to the point when the antioxidants were exhausted, as observed by the TBARS assay.

Toxicity and cellular uptake of EC and EC–PLGA Nanoparticles. Toxicity of EC and EC PLGA nanoparticles were evaluated by using HepG2 cell line (human hepatic carcinoma cells). The size of the EC and EC–PLGA nanoparticles did not significantly changed when the nanoparticles were suspended in the HepG2 cells growth medium for toxicity and cellular uptake assays (data not shown). The toxic concentration for this cell line was 165 μM for EC–PLGA nanoparticles and 386 μM for EC nanoparticles, defined as the EC concentration at which a 10% increase in absorbance was observed when compared to the control. Higher EC concentrations were tolerated in EC nanostructure form by HepG2 cells compared to EC–PLGA nanoparticles due to PLGA contribution to the toxicity levels. Both systems tested had the same EC concentrations.

Fluorescent nanoparticles made with the polymer (PLGA) covalently linked with a red fluorescent probe (TRITC) and the antioxidant surfactant (EC) were internalized by HepG2 cells over the course of the study, as

TABLE 1. Fluorescence Measurements of Three Different Sections Selected from Figure 12

time (min)	cell cluster (a.u.)	individual cell (a.u.)	no cells (a.u.)
preinoculation	12.84	22.54	9.16
0	20.27	101.42	24.28
5	23.28	93.97	14.16
60	33.65	116.90	14.26

showed by the increase in fluorescence intensity over the control (Figure 13A) from time 0 (Figure 13B) to 5 min (Figure 13C), 60 min (Figure 13D) and 150 min (Figure 13E). Cells internalized EC–PLGA–TRITC nanoparticles and fluorescence increased over time in selected cytoplasmatic regions of a family of cells and that of an individual cell (Table 1). Intensity measurements in areas without cells showed a decrease in intensity over time, from 24.28 (after nanoparticles inoculation, time 0) to 14.26 (60 min), as the particles were internalized by the cells, reducing the free EC–PLGA–TRITC nanoparticles available in the culture media.

CONCLUSIONS

A new antioxidant surfactant made of vitamin E and vitamin C was successfully synthesized, and it was used to form PLGA polymeric nanoparticles of antioxidant properties. EC was hydrophobic with a good solubility in polar solvents. Nanoprecipitation technique was successfully used to synthesize self-assembled EC and Span80 nanostructures, as well as polymeric PLGA–Span 80 and PLGA–EC nanoparticles. EC nanostructures were spherical and measured between 12 and 140 nm depending on the salt and surfactant concentration. Smaller EC nanostructures (12 ± 2 nm) were obtained when sodium bicarbonate was used in the aqueous phase. The polydispersity index was smaller for particles made in NaCl, and measured 0.27–0.18 at 1.5 to 99 mM NaCl concentration, as compared to values of 0.58–0.52 for the same concentration range in sodium bicarbonate. Span80 formed vesicles of 136–460 nm, with a polydispersity index representative of a monodisperse suspension. PLGA polymeric nanoparticle synthesized with the synthetic hydrophobic Span80 surfactant showed a bigger particle size (180 ± 12 to 216 ± 27 nm) as compared to the PLGA–EC nanoparticles (90 ± 5 to 126 ± 4 nm). Polymeric PLGA–EC nanoparticles showed an antioxidant activity (IC_{50} of 36.3 to 42.1 mM as measured by DPPH assay). The capacity to provide antioxidant action was provided by the vitamin C moiety of the EC surfactant which localized at the interface between the PLGA hydrophobic core and water. In comparison, PLGA–Span80 particles did not show any antioxidant activity. The antioxidant activity of EC and EC–PLGA nanoparticles was confirmed by EPR measurements. Even though the scavenging activity of EC was about twice higher than that of EC–PLGA NPs, the antioxidant properties were in a similar range. The TBARS assay showed that EC antioxidant surfactant protected linolenic acid against oxidation induced with AAPH (lag phase of 70 min). Interestingly, the PLGA–EC and PLGA-α-tocopherol nanoparticle systems presented higher lag phases suggesting better antioxidant behavior compared with the antioxidant solubilized in water (vitamin C) and the emulsion (α-tocopherol), respectively. The data suggested that the PLGA nanoparticle role is beyond the antioxidant action of the EC and α-tocopherol molecules, so the pro-oxidant role of antioxidants plus increased reaction speed to free radicals can provide better antioxidant performance in lipid peroxidation assays. The localization of antioxidant is important (hydrophilic or hydrophobic phase), but the structure and localization of the radicals byproduct is important too (stacked together in a system or in solution). EC–PLGA nanoparticles were internalized by HepG2 cells, and the nanoparticles were localized in the cytoplasm. The EC–PLGA nanoparticles uptake started as soon the nanoparticles were inoculated in the cell cultures, and it increased over time. The newly synthesized EC surfactant was therefore found successful in forming polymeric nanoparticles of intrinsic antioxidant properties. Further studies will be addressing the role of the polymeric antioxidant nanoparticles in cells and animal models.

EXPERIMENTAL SECTION

Materials. Poly(lactide-*co*-glycolide acid) (PLGA) 50:50, molecular weight 30000–75000 g/mol, ascorbic acid, α-tocopherol, 2,2-diphenyl-1-picrylhydrazyl (DPPH), 5,6-isopropylideneascorbic acid, α-tocopherol, ethyl chloroformate, maleic anhydride, polyvinyl alcohol (PVA) 87–89% hydrolyzed (31000–50000 g/mol), 2,2′-azobis(2-methylpropionamidine) dihydrochloride (AAPH), 2,6-di-*tert*-butyl-4-methylphenol (BHT), ethylenediaminetetraacetic acid (EDTA), tris(hydroxymethyl)aminomethane (Tris-HCl), linolenic acid, Tween 20, 2-thiobarbituric acid (TBA), trichloroacetic acid (TCA), 1,1,3,3-tetramethoxypropane, dicyclohexylcarbodiimide (DCC), *N*-hydroxysuccinimide (NHS), tetramethylrhodamine-5-isothiocyanate (TRITC), ethylenediamine, α-tocopherol, vitamin C, anhydrous sodium acetate, ethanol, dichloromethane (DCM), dimethyl sulfoxide (DMS), glutaraldehyde, methylene blue, Hanks' Balanced Salt Solution (HBSS), acetic acid, and phosphate buffered solution (PBS) were purchased from Sigma-Aldrich (St. Louis, MO). Acetone, ethanol, 1-propanol, hexane, acetonitrile, diethyl ether chloroform, ethyl acetate were HPLC grade (Mallinckrodt Baker, Pittsburgh, NJ). Human liver carcinoma cell (HepG2) was supplied by ATCC. Williams' Medium E (WME) was purchased from Invitrogen. Fetal bovine serum (FBS) was obtained from Atlanta Biologicals.

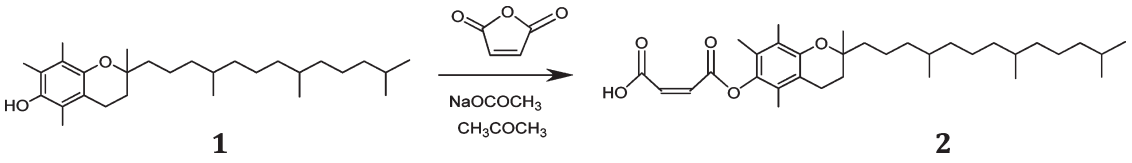

Scheme 1. Synthesis of maleic acid mono-α-tocopherol (2).

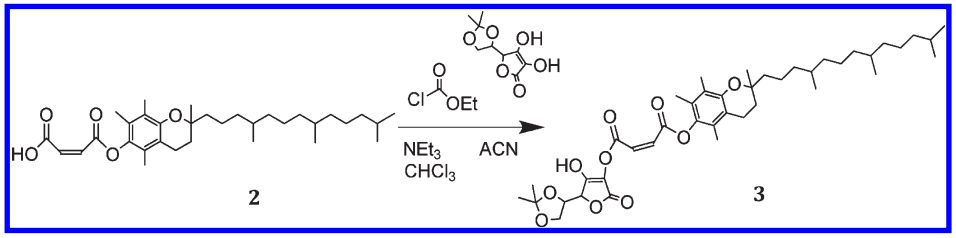

Scheme 2. Synthesis of 5,6-isopropylideneascorbic acid-2-*O*-maleic acid-α-tocopherol diester (3).

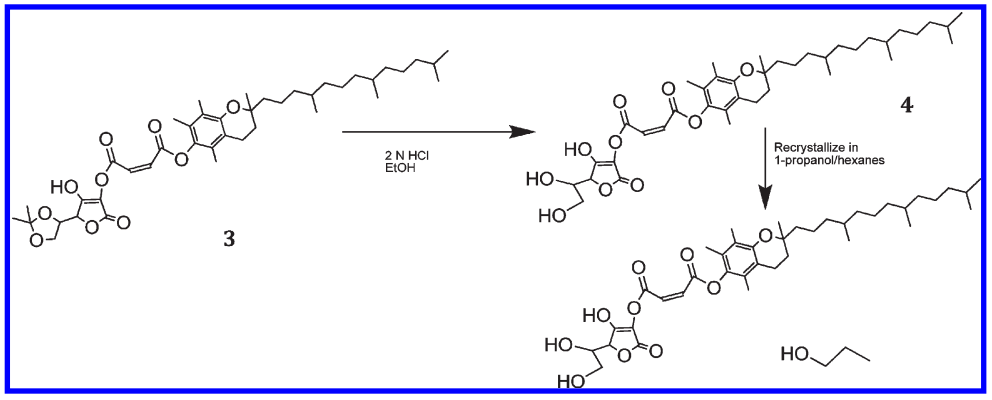

Scheme 3. Synthesis of L-ascorbic acid-2-*O*-maleic acid-α-tocopherol diester (4).

Synthesis of Vitamin E–C Surfactant. The synthesis of vitamin E–C was performed in four steps (see Schemes 1, 2, and 3) following a procedure similar to that described by Ogata and co-workers.[44]

α-Tocopherol (**1**) (10.2 g, 0.024 mol), maleic anhydride (6.3 g, 0.064 mol), and anhydrous sodium acetate (3.2 g, 0.39 mol) were placed in 65 mL of reagent grade acetone in a 100 mL round-bottomed flask and heated at reflux with stirring for 1 h. The acetone was then removed by rotary evaporation. The reaction mixture was dissolved in 100 mL of diethyl ether, and aqueous saturated ammonium chloride solution (50 mL) was added. This solution was stirred at room temperature for 20 min. The aqueous layer was removed and the organic layer was washed with water (2 × 100 mL). The ether layer was dried over $MgSO_4$ and filtered, and the ether was removed by rotary evaporation to yield a golden-orange oil which slowly crystallizes (12.0 g, 96%). No further purification techniques were performed as the compound decomposes on silica gel. ^{1}H NMR (300 MHz, CDCl3) δ0.84 (s), 0.87 (s), 0.88 (s), 0.89 (s), 0.97–1.18 (br m), 1.26 (br s), 1.28–1.40 (br m), 1.49–1.59 (br m), 1.70–1.90 (br m), 2.00 (s), 2.04 (s), 2.12 (s), 2.62 (br t, *J* = 9 Hz), 6.65 (1H, d, *J* = 13 Hz), 6.71 (1 H, d, *J* = 13 Hz). ^{13}C NMR (75.5 MHz, CDCl3) δ11.91, 12.20, 13.04, 19.64, 19.71, 19.78, 20.61, 21.03, 22.66, 22.76, 24.46, 24.83, 28.00, 32.69, 32.80, 37.28, 37.35, 37.39, 37.45, 37.51, 39.37, 75.33, 117.69, 123.47, 124.37, 125.98, 128.07, 137.67, 139.74, 150.03, 164.68, 166.32.

Maleic acid mono-α-tocopherol (**2**) (6.3 g, 0.012 mol), triethylamine (4.1 g, 0.041 mol), and chloroform (33 mL) were combined in a 100 mL round-bottomed flask fitted with a septum and cooled to 0 °C on an ice bath. Ethylchloroformate (2.0 g, 0.018 mol) was added dropwise. The reaction mixture was stirred at 0 °C for 10 min. 5,6-Isopropylideneascorbic acid (3.6 g, 0.017 mol) in 45 mL of acetonitrile was quickly added, and the solution was stirred at 0 °C for 15 min and then warmed to 5 °C over a 30 min period with continued stirring. The solvent was then removed by rotary evaporation at room temperature. The reaction residue was then taken up in 40 mL of ethyl acetate, and this organic solution was washed with 2 N HCl (9.8 mL) and then with water (2 × 25 mL). The ethyl acetate solution was dried over $MgSO_4$, filtered, and the solvent was removed by rotary evaporation. This yielded a golden oil (**3**) (6.6 g, 76%). The compound was not further purified as it decomposed on contact with silica gel. ^{1}H NMR on crude product (300 MHz, CDCl3) δ0.86 (s), 0.87 (s), 0.90 (s), 0.89 (s), 1.10–1.19 (br m), 1.24–1.27 (br m), 1.36 (s), 1.40 (s), 1.50–1.58 (br m), 1.74–1.86 (br m), 2.00 (s), 2.04 (s), 2.11 (s), 2.60 (br t, *J* = 6 Hz), 4.13 (sextet, *J* = 7 Hz), 4.38 (m), 4.70 (d, *J* = 3 Hz), 6.67 (s).

5,6-Isopropylideneascorbic acid-2-*O*-maleic acid-α-tocopherol diester (**3**) (6.6 g, 0.0091 mol) was placed in 28 mL of ethanol and 8 mL of 2 N HCl solution. This solution was stirred at 60 °C for 25 min. The ethanol was removed by rotary evaporator and the remaining residue was dissolved in 35 mL of ethyl acetate. This was washed with water (2 × 10 mL). The ethyl acetate layer was dried with $MgSO_4$, filtered, and the solvent was removed by rotary evaporation. The resulting oil (**4**) was dissolved in 8.3 mL of 1-propanol and 19 mL of hexanes. The solution was placed in the freezer overnight and crystals were collected by suction filtration. The crystals were recrystallized in 1:3 (v/v) 1-propanol: hexanes solution to yield a first crop of very light yellow solid (**4**) which were dried for 7 h under vacuum at room temperature (0.639 g, 10%). ^{1}H NMR (300 MHz, d6-DMSO) δ0.80 (s), 0.82 (s), 0.83 (s), 0.84 (s), 0.85 (s), 0.95–1.13 (br m), 1.18–1.24 (br m), 1.35–1.55 (br m), 1.73 (br t), 1.95 (s), 1.97 (s), 2.01 (s), 2.55 (br t), 3.33 (t, *J* = 7 Hz), 3.81 (t, *J* = 7 Hz), 4.95 (s), 6.66 (d, *J* = 12 Hz), 7.08

(d, J = 12 Hz). ^{13}C NMR (75.5 MHz, CDCl3) δ10.52, 11.64,12.02, 12.88, 19.54, 19.62, 19.65, 19.68, 20.00, 22.52, 22.61, 23.80, 24.25, 25.70, 28.85, 32.04, 32.09, 32.13, 36.67, 36.75, 36.78, 36.83, 38.84, 61.74, 62.52, 68.63, 74.84, 74.86, 75.54, 111.71, 117.09, 117.40, 121.89, 125.23, 126.56, 139.64, 148.82, 161.23, 163.42, 164.26, 167.41.

Nanoparticle Synthesis. EC and Span80 nanostructures in the absence or in the presence of poly(lactic-*co*-glycolic acid) were synthesized by a modified version of the nanoprecipitation method. An organic phase was made of acetone (0.5 mL) with dissolved PLGA (0−1.2 mg/mL) -when the polymer was used, and EC surfactant or Span80 (at various concentrations, 1 to 5 mg/mL). The organic phase was added to 5 mL of nanopure water (Thermo Scientific Barnstead Nanopure, Dubuque, IA) by a syringe under stirring on a magnetic stir plate (Corning, NY). Next, the sample was placed in a Buchi R-124 rotoevaporator (Buchi Corporation, New castle, DE) to remove the organic solvent, acetone. Evaporation was performed for 10 min under vacuum and nitrogen injection for fast solvent evaporation. The nanoparticle suspension was collected and stored for further analysis at 4 °C, under dark conditions.

PLGA-TRITC (Tetramethylrhodamine-5-isothiocyanate) Synthesis. For the cellular uptake study of EC−PLGA nanoparticles fluorescent PLGA was synthesized by coupling the dye TRITC with PLGA by carbodiimide chemistry. Briefly, 200 mg of PLGA was dissolved in anhydrous DCM (8 mL). Next, PLGA was activated by adding DCC (20 μmol) and NHS (20 μmol) at room temperature for 8 h. After, the byproduct *N,N′*-dicyclohexylurea was removed by filtration. The pure activated PLGA was reacted with 10-fold excess molar amount of ethylenediamine (3.3 μL, 50 μmol) in 10 mL DCM at room temperature for 8 h and further purified by precipitation in cold diethyl ether and dry under vacuum. The dye, TRITC (3.6 mg, 7.5 μmol) was added to the amine terminated PLGA (100 mg) in DMSO (5 mL) at room temperature for 8 h. The final product was precipitated 10 times in excess ethanol to remove unreacted TRITC and dried under high vacuum.[45]

Size, Size Distribution, and Zeta-Potential. The nanoparticle size and polydispersity index (PI) were evaluated by dynamic light scattering (DLS) using a Malvern Zetasizer Nano ZS (Malvern Instruments, Ltd., Worcestershire, UK). Zeta potential measurements were obtained by Malvern Zetasizer Nano ZS with a MPT-2 autotritator required to study aggregation of particles against pH. The samples were diluted to a final concentration range of 0.1 mg/mL for all measurements.

Morphology of Antioxidant Nanoparticles. Transmission electron microscopy (TEM) with a JEOL 100-CX (JEOL USA Inc., Peabody, MA) microscope was used to study nanoparticle morphology. A droplet of the sample was mixed with a contrast agent (Uracyl acetate, 2%) and a carbon grid was passed on the surface of the droplet to create a film over the grid. The sample was placed in the TEM after 15 min for analysis.

DPPH Radical Scavenging Assay Method. A stock solution of DPPH in methanol at 0.4 mM was prepared and kept at −20 °C in the dark prior to use. The nanoparticle sample was diluted with acetic acid solution to 1 mL. The nanoparticle sample was added to dilute DPPH stock in methanol to obtain a final sample volume of 2 mL with a 0.1 mM DPPH concentration. The ratio between water and methanol was 1:1 v/v. The blank was prepared with 1 mL of acetic acid solution and pure methanol. The controls were prepared for each sample, with 1 mL of acetic solution and 1 mL of DPPH in methanol solution. Absorption readings were taken after 30 min at 518 nm using a Geminys 6 spectrophotometer (Thermo Scientific, Waltham, MA). The formula used to calculate the rate of oxidation was

$$\%\ \text{changeinactivity} = ((\text{Abs}_{\text{control}} - \text{Abs}_{\text{sample}})/\text{Abs}_{\text{control}})100 \quad (1)$$

The measurements were performed at five nanoparticle concentrations (0.025−0.1 mM). The data collected were used to obtain the best fit for the linear regression performed in order to estimate the IC_{50} (inhibitory concentration), which is the point at which 50% of the molecules had been oxidized. Antioxidant activity of EC was measured at the same concentrations used for the nanoparticles synthesis. It was assumed that EC was uniformly distributed on the surface of the PLGA−EC nanoparticles.

DPPH Radical Scavenging Measurements by Electron Paramagnetic Resonance (EPR) Technique. The DPPH radical is widely used as a test radical to assess antioxidant capacity and activity of organic compounds. The EPR spectroscopy is one of the most sensitive techniques to detect and follow the behavior of the DPPH radical directly. Scavenging of the DPPH radical was followed by measuring the decrease in the EPR signal intensity.

EPR measurements were conducted on a Bruker EMX-20/2.7 EPR spectrometer (X-band) with dual cavities, modulation and microwave frequencies of 100 kHz and 9.516 GHz, respectively. The typical parameters were sweep width, 100 G; EPR microwave power of 10 mW; and modulation amplitude, 2.5 G. Time constant and sweep time were varied. Values of *g*-factors were calculated using Bruker's WINEPR program which is a comprehensive line of software, allowing control of the Bruker EPR spectrometer, data-acquisition, automation routines, tuning, and calibration [http://us.bruker-biospin.com/brukerepr/winepr.html].

The samples were prepared in the same way as described in the DPPH assay method. The following solutions were subjected to the EPR examination: EC (0.1 mM) mixed with DPPH (0.1 mM) at a ratio of 1:1, EC−PLGA nanoparticles (NP) (0.1 mM EC) mixed with DPPH (0.1 mM) at a ratio of 1:1. As a reference, 0.1 mM DPPH in 1:1 methanol/water solution was used. The solutions were prepared right before EPR measurements. A 30 μL sample was transferred into a EPR capillary tube (i.d. $\approx$ 1 mm, o.d. $\approx$ 1.55 mm) and the end was sealed by a critoseal (Fisherbrand). Then, the capillary was inserted in an ordinary 4 mm EPR tube and was placed into the EPR resonator to measure the EPR spectra of the DPPH radicals over time. The delay time was between 1 and 2 min after mixing of EC or NP with DPPH before the first EPR measurement was performed.

A kinetic measurement of DPPH radical scavenging upon mixing of EC (or NP) with DPPH was also performed. A volume of 30 μL sample was transferred into the EPR tube (o.d. = 3 mm, i.d. = 2 mm), positioned in the cavity, and the same quantity of DPPH was injected rapidly to the solution by syringe through the tiny PVC hose (i.d. = 0.3 mm) located directly in solution (close to the bottom of EPR tube).

The magnetic field was fixed at a specified value (at the strongest peak of the DPPH radical), and the EPR signal intensity was monitored as a function of time (Figure 9, top line).

Thiobarbituric Acid Reactive Substances (TBARS) Assay. TBARS assay has been widely used to study the lipid peroxidation processes and antioxidant action of different antioxidants.[40,46−48] The substrate used was linolenic acid which was emulsified with Tween 20. The first step was to dissolve an amount of linolenic acid (10 mM final concentration) in acetone (1 mL), which was added to an aqueous solution of Tris-HCl (adjusted to pH 7.3 with HCl) and Tween 20 (4.6 mg/mL). The organic phase was slowly added with a syringe under stirring. The final volume was 19 mL after solvent evaporation in a Buchi R-124 rotoevaporator. When EC nanoparticles were formed, EC was added in the organic phase (acetone) for a final concentration of 150 μM, and the same procedure described above was followed. The PLGA−EC nanoparticles were synthesized by the nanoprecipitation technique in which PLGA and EC were added to the organic phase. The EC final concentration used in the experiments was 150 μM. The PLGA entrapped vitamin E nanoparticles were synthesized by an emulsion-evaporation technique in which the PLGA and α-tocopherol (final concentration of 50 μM) were dissolved in dichloromethane, and the aqueous phase was formed by 0.3% PVA. The solvent evaporation was performed by a rotovap under vacuum and nitrogen injection for 6 min. The oxidation of linolenic acid (10 mM final concentration) was started with a hydrophilic initiator (AAPH) (10 mM final concentration), and the temperature was kept constant at 37 °C. The PLGA polymeric systems were added to the aqueous phase. Vitamin C antioxidant was added to the aqueous phase to evaluate its performance. When the antioxidant was mixed with linolenic acid, the addition of antioxidants was performed in the organic phase. Emulsion samples of 0.6 mL were mixed with 0.6 mL of TBARS solution (A 100 mL mixture of thiobarbituric acid 0.67%, 10% trichloroacetic acid, and 0.25 M HCl was

prepared fresh for each experiment), and 0.1 mL of a mixture of BHT (10 mM) and EDTA (5 mM) to stop oxidation after sampling. The samples were heated at 90 °C for 40 min in an oven. After, the vial samples were cooled down and centrifuged for 30 min at 10000*g* (Beckman Coulter, Allegra 64R). Finally, the supernatant was collected, and absorbance was measured at 535 nm.

Cell Culture. HepG2 cells were cultured in growth medium (WME supplemented with 5% FBS, 10 mM Hepes, 2 mM L-glutamine, 5 μg/mL insulin, 0.05 μg/mL hydrocortisone, 50 units/mL penicillin, 50 μg/mL streptomycin, and 100 μg/mL gentamicin or MEM supplemented with 10% FBS) while at 37 °C and 5% CO_2, modified from Wolfe and Liu 2007.[49] Cells used in this study were between passages 80 and 92.

Cytotoxicity Study. Nanoparticle cytotoxicity was gauged *via* a modified method by Wolfe and Liu 2007.[49] HepG2 cells were seeded at 10^4/well on a 96-well plate in 100 μL of growth medium (WME supplemented with 5% FBS, 10 mM Hepes, 2 mM L-glutamine, 5 μg/mL insulin, 0.05 μg/mL hydrocortisone, 50 units/mL penicillin, 50 μg/mL streptomycin, and 100 μg/mL gentamicin) and incubated for 24 h at 37 °C. After the medium was removed, varied concentrations of EC and EC−PLGA nanoparticles in 100 μL of treatment medium were applied to the cells in triplicate wells. The plates were then incubated at 37 °C for 24 h. Cells were washed with PBS after the treatment medium was removed; 50 μL/well methylene blue staining solution (98% HBSS, 0.67% glutaraldehyde, 0.6% methylene blue) was applied to each well, and the plate was incubated at 37 °C for 1 h. The dye was removed, and the plate was rinsed with nanopure water until the water ran clear. The plate was tapped to remove water from all wells and allowed to air-dry. A 100 μL portion of elution solution (49% PBS, 50% ethanol, 1% acetic acid) was added to each well. Immediately following, the microplate was placed on a benchtop shaker for 20 min for uniform elution. Absorbance readings were taken at 570 nm with blank subtraction using a Benchmark Plus Microplate spectrophotometer (Bio-Rad Laboratories Ltd., UK). Nanoparticle concentrations that increased the absorbance by >10% when compared to the control were considered to be cytotoxic.[49]

Cell Uptake Microscopy. Cell uptake was measure qualitatively by confocal microscopy and analyzed quantitatively. HepG2 cells were seeded at 5×10^4/well on an 8-well plate (Labtek) in 500 μL of growth medium (Minimum Essential Medium (MEM) supplemented with 10% FBS) and incubated for 24 h at 37 °C. Untreated cells were imaged for control. Cells were then treated with 17 μL of EC−PLGA−TRITC nanoparticles/well in growth medium and immediately imaged at time zero. Cells were imaged again at times 0, 5, 60, and 150 min after inoculation. The fluorescence dye used was tetramethylrhodamine-5-isothiocyanate (TRITC) which was covalently linked to PLGA to obtain fluorescence PLGA. The PLGA−TRITC nanoparticles were formed as described in Nanoparticle Synthesis.

Statistical Analysis. The statistical analysis was performed with SAS (Cary, NC). *Anova proc* mixed procedure with Tukey adjustment was used and significant differences were declared at a *p* value of 0.05. All the analyses were performed in triplicate.

Acknowledgment. Thanks go to C. Henk and M. Brown at the Socolofsky Microscopy Center at LSU for their support in acquiring the TEM and the confocal microscopy pictures, and K. C. McDonough for her advice and work in the cellular studies. This work was supported by the American Chemical Society PRF-G Program.

REFERENCES AND NOTES

1. Chiellini, E.; Chiellini, E. E.; Chiellini, F.; Solaro, R. Targeted Administration of Proteic Drugs. I. Preparation of Polymeric Nanoparticles. *J. Bioact. Compat. Polym.* **2001**, *16*, 441–465.
2. Astete, C. E.; Sabliov, C. M. Synthesis and Characterization of Plga Nanoparticles. *J. Biomater. Sci., Polym. Ed.* **2006**, *17*, 247–289.
3. Kreuter, J. Nanoparticles and Microparticles for Drug and Vaccine Delivery. *J. Anat.* **1996**, *189*, 503–505.
4. Damge, C.; Vranckx, H.; Balschmidt, P.; Couvreur, P. Poly-(Alkyl Cyanoacrylate) Nanospheres for Oral Administration of Insulin. *J. Pharm. Sci.* **1997**, *86*, 1403–1409.
5. Mukerjee, A.; Pruthi, V. Oral Insulin Delivery by Polymeric Nanospheres. *J. Biomed. Nanotechnol.* **2007**, *3*, 68–74.
6. Rawat, M.; Singh, D.; Saraf, S.; Saraf, S. Nanocarriers: Promising Vehicle for Bioactive Drugs. *Biol. Pharm. Bull.* **2006**, *29*, 1790–1798.
7. Agarwal, A.; Saraf, S.; Asthana, A.; Gupta, U.; Gajbhiye, V.; Jain, N. K. Ligand Based Dendritic Systems for Tumor Targeting. *Int. J. Pharm.* **2008**, *350*, 3–13.
8. Kreuter, J. Drug Targeting with Nanoparticles. *Eur. J. Drug Metab. Pharmacokinet.* **1994**, *19*, 253–256.
9. Rawat, A.; Vaidya, B.; Khatri, K.; Goyal, A. K.; Gupta, P. N.; Mahor, S.; Paliwal, R.; Rai, S.; Vyas, S. P. Targeted Intracellular Delivery of Therapeutics: An Overview. *Pharmazie* **2007**, *62*, 643–658.
10. Hammady, T.; Rabanel, J. M.; Dhanikula, R. S.; Leclair, G.; Hildgen, P. Functionalized Nanospheres Loaded with Anti-angiogenic Drugs: Cellular Uptake and Angiosuppressive Efficacy. *Eur. J. Pharm. Biopharm.* **2009**, *72*, 418–427.
11. Zhao, X. B.; Li, H.; Lee, R. J. Targeted Drug Delivery *via* Folate Receptors. *Expert Opin. Drug Delivery* **2008**, *5*, 309–319.
12. Reddy, M. K.; Wu, L.; Kou, W.; Ghorpade, A.; Labhasetwar, V. Superoxide Dismutase-Loaded PLGA Nanoparticles Protect Cultured Human Neurons under Oxidative Stress. *Appl. Biochem. Biotechnol.* **2008**, *151*, 565–577.
13. Schaffazick, S. R.; Siqueira, I. R.; Badejo, A. S.; Jornada, D. S.; Pohlmann, A. R.; Netto, C. A.; Guterres, S. S. Incorporation in Polymeric Nanocapsules Improves the Antioxidant Effect of Melatonin against Lipid Peroxidation in Mice Brain and Liver. *Eur. J. Pharm. Biopharm.* **2008**, *69*, 64–71.
14. Simone, E. A.; Dziubla, T. D.; Arguiri, E.; Vardon, V.; Shuvaev, V. V.; Christofidou-Solomidou, M.; Muzykantov, V. R. Loading Peg-Catalase into Filamentous and Spherical Polymer Nanocarriers. *Pharm. Res.* **2009**, *26*, 250–260.
15. Williams, S. R.; Lepene, B. S.; Thatcher, C. D.; Long, T. E. Synthesis and Characterization of Poly(Ethylene Glycol)−Glutathione Conjugate Self-Assembled Nanoparticles for Antioxidant Delivery. *Biomacromolecules* **2009**, *10*, 155–161.
16. Nie, Z.; Liu, K. J.; Zhong, C. J.; Wang, L. F.; Yang, Y.; Tian, Q.; Liu, Y. Enhanced Radical Scavenging Activity by Antioxidant-Functionalized Gold Nanoparticles: A Novel Inspiration for Development of New Artificial Antioxidants. *Free Radical Biol. Med.* **2007**, *43*, 1243–1254.
17. Lee, B. S.; Yuan, X.; Xu, Q.; Mclafferty, F. S.; Petersen, B. A.; Collette, J. C.; Black, K. L.; Yu, J. S. Preparation and Characterization of Antioxidant Nanospheres from Multiple Alpha-Lipoic Acid-Containing Compounds. *Bioorg. Med. Chem. Lett.* **2009**, *19*, 1678–1681.
18. Sabliov, C. M.; Astete, C. E. Encapsulation and Controlled Release of Antioxidants and Vitamins. In *Delivery and Controlled Release of Bioactives in Foods and Nutraceuticals*; Garti, N., Ed.; CRC Press: New York, 2008; pp 297−330.
19. Brigelius-Flohe, R.; Traber, M. G. Vitamin E: Function and Metabolism. *FASEB J.* **1999**, *13*, 1145–1155.
20. Traber, M. G.; Atkinson, J. Vitamin E, Antioxidant and Nothing More. *Free Radical Biol. Med.* **2007**, *43*, 4–15.
21. Halliwell, B. Antioxidants in Human Health and Disease. *Annu. Rev. Nutr.* **1996**, *16*, 33–50.
22. Denisov, E. T.; Afanasev, I. B. In *Oxidation and Antioxidants in Organic Chemistry and Biology*; Taylor & Francis: Boca Raton, FL; 2005;
23. Halliwell, B.; Gutteridge, J. M. C. In *Free Radicals in Biology and Medicine*; Oxford University Press: New York; 1999;
24. Halliwell, B. Vitamin C: Antioxidant or Pro-Oxidant *in Vivo*. *Free Radical Res.* **1996**, *25*, 439–454.
25. Noguchi, N.; Iwaki, Y.; Takahashi, M.; Komuro, E.; Kato, Y.; Tamura, K.; Cynshi, O.; Kodama, T.; Niki, E. 2,3-Dihydro-5-hydroxy-2,2-dipentyl-4,6-di-*tert*-butylbenzofuran: Design and Evaluation as a Novel Radical-Scavenging Antioxidant against Lipid Peroxidation. *Arch. Biochem. Biophys.* **1997**, *342*, 236–243.

26. Chabrier, P. E.; Auguet, M.; Spinnewyn, B.; Auvin, S.; Cornet, S.; Demerle-Pallardy, C.; Guilmard-Favre, C.; Marin, J. G.; Pignol, B.; Gillard-Roubert, V.; *et al.* BN 80933, a Dual Inhibitor of Neuronal Nitric Oxide Synthase and Lipid Peroxidation: A Promising Neuroprotective Strategy. *Proc. Natl. Acad. Sci. U.S.A.* **1999**, *96*, 10824–10829.
27. Capuzzi, G.; Lonostro, P.; Kulkarni, K.; Fernandez, J. E. Mixtures of Stearoyl-6-*O*-Ascorbic Acid and α-Tocopherol: A Monolayer Study at the Gas/Water Interface. *Langmuir* **1996**, *12*, 3957–3963.
28. Rezk, R. M.; Haenen, G. R. M. M.; Van Der Vijgh, W. J. F.; Bast, A. The Extraordinary Antioxidant Activity of Vitamin E Phosphate. *BBA-Mol. Cell Biol. L.* **2004**, *1683*, 16–21.
29. Iuliano, L.; Pedersen, J. Z.; Camastra, C.; Bello, V.; Ceccarelli, S.; Violi, F. Protection of Low Density Lipoprotein Oxidation by the Antioxidant Agent Irfi005, a New Synthetic Hydrophilic Vitamin E Analogue. *Free Radical Biol. Med.* **1999**, *26*, 858–868.
30. Rosenau, T.; Adelwohrer, C.; Kloser, E.; Mereiter, K.; Netscher, T. Bromination of α-Tocopherol Methano-dimer and Ethano-dimer. *Tetrahedron* **2006**, *62*, 1772–1776.
31. Rosenau, T.; Habicher, W. D. "Vitamin CE," a Novel Prodrug Form of Vitamin E. *Chem. Pharm. Bull. (Tokyo)* **1997**, *45*, 1080–1084.
32. Tafazoli, S.; Wright, J. S.; O'brien, P. J. Prooxidant and Antioxidant Activity of Vitamin E Analogues and Troglitazone. *Chem. Res. Toxicol.* **2005**, *18*, 1567–1574.
33. Campo, G. M.; Ceccarelli, S.; Squadrito, F.; Altavilla, D.; Dorigotti, L.; Caputi, A. P. Raxofelast (IRFI 016): A New Hydrophilic Vitamin E-like Antioxidant Agent. *Cardiovasc. Drug Rev.* **1997**, *15*, 157–173.
34. Morley, S.; Cross, V.; Cecchini, M.; Nava, P.; Atkinson, J.; Manor, D. Utility of a Fluorescent Vitamin E Analogue as a Probe for Tocopherol Transfer Protein Activity. *Biochemistry (Wash.)* **2006**, *45*, 1075–1081.
35. Lo Nostro, P.; Ramsch, R.; Fratini, E.; Lagi, M.; Ridi, F.; Carretti, E.; Arnbrosi, M.; Ninham, B. W.; Baglioni, P. Organogels from a Vitamin C-Based Surfactant. *J. Phys. Chem. B* **2007**, *111*, 11714–11721.
36. Quintanarguerrero, D.; Allemann, E.; Doelker, E.; Fessi, H. A Mechanistic Study of the Formation of Polymer Nanoparticles by the Emulsification-Diffusion Technique. *Colloid Polym. Sci.* **1997**, *275*, 640–647.
37. Bohmer, M. R.; Koopal, L. K.; Lyklema, J. Micellization of Ionic Surfactants—Calculations Based on a Self-Consistent Field Lattice Model. *J. Phys. Chem. A* **1991**, *95*, 9569–9578.
38. Griffiths, P. C.; Paul, A.; Heenan, R. K.; Penfold, J.; Ranganathan, R.; Bales, B. L. Role of Counterion Concentration in Determining Micelle Aggregation: Evaluation of the Combination of Constraints from Small-Angle Neutron Scattering, Electron Paramagnetic Resonance and Time-Resolved Fluorescence Quenching. *J. Phys. Chem. B* **2004**, *108*, 3810–3816.
39. Vlachy, N.; Drechsler, M.; Verbavatz, J. M.; Touraud, D.; Kunz, W. Role of the Surfactant Headgroup on the Counterion Specificity in the Micelle-to-Vesicle Transition through Salt Addition. *J. Colloid Interface Sci.* **2008**, *319*, 542–548.
40. Puhl, H.; Waeg, G.; Esterbauer, H. Methods to Determine Oxidation of Low-Density Lipoproteins. *Method. Enzymol.* **1994**, *233*, 425–441.
41. Bowry, V. W.; Stocker, R. Tocopherol-Mediated Peroxidation—The Prooxidant Effect of Vitamin-E on the Radical-Initiated Oxidation of Human Low-Density-Lipoprotein. *J. Am. Chem. Soc.* **1993**, *115*, 6029–6044.
42. Bowry, V. W.; Mohr, D.; Cleary, J.; Stocker, R. Prevention of Tocopherol-Mediated Peroxidation in Ubiquinol-10-Free Human Low-Density-Lipoprotein. *J. Biol. Chem.* **1995**, *270*, 5756–5763.
43. Mukai, K.; Morimoto, H.; Okauchi, Y.; Nagaoka, S. Kinetic-Study of Reactions between Tocopheroxyl Radicals and Fatty-Acids. *Lipids* **1993**, *28*, 753–756.
44. Ogata, K.; Saito, N.; Yamada, K.; Maruyama, G. U.S. Patent 6,828,348 2004.
45. Chung, Y. I.; Kim, J. C.; Kim, Y. H.; Tae, G.; Lee, S. Y.; Kim, K.; Kwon, I. C. The Effect of Surface Functionalization of PLGA Nanoparticles by Heparin- or Chitosan-Conjugated Pluronic on Tumor Targeting. *J. Controlled Release* **2010**, *143*, 374–382.
46. Esterbauer, H.; Cheeseman, K. H. Determination of Aldehydic Lipid-Peroxidation Products—Malonaldehyde and 4-Hydroxynonenal. *Method. Enzymol.* **1990**, *186*, 407–421.
47. Huber, G. M.; Rupasinghe, H. P. V.; Shahidi, F. Inhibition of Oxidation of Omega-3 Polyunsaturated Fatty Acids and Fish Oil by Quercetin Glycosides. *Food Chem.* **2009**, *117*, 290–295.
48. Lukaszewicz, M.; Szopa, J.; Krasowska, A. Susceptibility of Lipids from Different Flax Cultivars to Peroxidation and Its Lowering by Added Antioxidants. *Food Chem.* **2004**, *88*, 225–231.
49. Wolfe, K. L.; Liu, R. H. Cellular Antioxidant Activity (CAA) Assay for Assessing Antioxidants, Foods, and Dietary Supplements. *J. Agric. Food Chem.* **2007**, *55*, 8896–8907.